Astronomy Reports, Vol. 47, No. 8, 2003, pp. 621–636. Translated from Astronomicheskiĭ Zhurnal, Vol. 80, No. 8, 2003, pp. 675–691.

Light Curve Interpretation for "Quiescent" X-ray Novae in a Model with Noncollisional Interaction between the Flow and Disk. The System GU Mus = GRS 1124–68

T. S. Khruzina[1], A. M. Cherepashchuk[1], D. V. Bisikalo[2], A. A. Boyarchuk[2], and O. A. Kuznetsov[2,3]

[1] *Sternberg Astronomical Institute, Universitetskiĭ pr. 13, Moscow, 119992 Russia*

[2] *Institute of Astronomy, Russian Academy of Sciences, ul. Pyatnitskaya 48, Moscow, 119017 Russia*

[3] *Keldysh Institute of Applied Mathematics, Russian Academy of Sciences, Miusskaya pl. 4, Moscow, 125047 Russia*

Received March 5, 2003; in final form, March 14, 2003

Abstract—We have analyzed optical and infrared light curves of GU Mus obtained during the system's quiescent state and carried out computations for "hot-line" and "hot-spot" models. The hot-line model describes the optical variability of GU Mus better than the hot-spot model. Season-to-season variations of the shape, amplitude, and mean levels of the optical and infrared light curves of GU Mus are due to changing parameters of the hot line and, to a lesser degree, of the accretion disk. Taking into account the contribution of the variability of the disk + hot line system to the variability of the system as a whole, we are able to reliably estimate the orbital inclination, $i = 54^\circ \pm 1\overset{\circ}{.}3$, and the mass of the black hole, $M_X = (6.7–7.6)\, M_\odot$.

1. INTRODUCTION

Among the numerous stellar X-ray sources, there exists a small group of stars whose members exhibit characteristic X-ray variations in which their X-ray luminosity increases by a factor of several hundred thousand within days, after which the luminosity returns to its original value over several months (cf., for example, [1, 2]). This behavior strongly resembles the light curves of classical novae, leading to these variable X-ray sources being named "X-ray novae." Subsequent optical observations of these objects have confirmed the novalike character of their outbursts.

Spectroscopic observations of such objects demonstrate that they were binaries, like classical or dwarf novae. The secondary, whose light dominates in the optical during quiescence, is usually a main-sequence star, subgiant, or even late-type giant. In contrast to the primaries of classical novae, which are white dwarfs, the primary is now a neutron star or black hole. Consequently, most of the gravitational energy released during accretion is emitted in the X-ray. More detail on the physics of X-ray novae can be found in the reviews [3–6] and the recent monograph [7].

The X-ray outbursts are accompanied by optical outbursts due to X-ray heating of the accretion disk and optical star, making it possible to identify X-ray novae very reliably. At the same time, the quiescent optical spectra of X-ray novae contain absorption lines of the optical star, enabling measurement of their mass function and estimation of the mass of the relativistic object (cf., for instance, the reviews [8, 9]).

During quiescence, the luminosity of the optical star is comparatively low. When interpreting the optical light curves of X-ray novae, it is necessary to take into account the effect of the optical star's ellipsoidal shape, the contribution of the accretion disk's radiation, and variability due to the contribution of light from the region where the disk interacts with the gas flow. The three-dimensional gas-dynamical computations of gas flows in interacting binary systems [10–13] have demonstrated that, in self-consistent flow models, the major region of energy release is located outside the disk, in a shock wave due to interaction of the flow with matter of the circumstellar envelope; this is the "hot-line" model. Application of the hot-line model to the interpretation of the optical and infrared light curves of dwarf novae [14–16] have illustrated its advantages over hot-spot models.

The current study is aimed at analyzing the light curves of the X-ray nova GU Mus in quiescence using the hot-line model.

1063-7729/03/4708-0621$24.00

2. GENERAL INFORMATION ABOUT THE X-RAY NOVA GU Mus

The X-ray nova Muscae 1991 GU Mus = XN Mus 1991 = GS 1124−683 = GRS 1124−68) was independently discovered in sky surveys by the GRANAT and GINGA space telescopes on January 9, 1991 [17, 18]. Four days later, it was identified with an optical star ($V = 13^m.0$) located near the X-ray source [19]. After another several days, the flux from the system had decreased to $V \sim 13^m.4$, and it had decreased to its pre-outburst level, $V \sim 20^m.5$, in about a year.

Remillard *et al.* [20] acquired photometric and spectroscopic observations of GU Mus at 4900−6500 Å and in the I filter 15 months after the outburst, when the system had returned to quiescence ($V \sim 20^m.5$). The spectrum appeared to correspond to a K0−K4V star. The half-amplitude of the secondary's radial-velocity curve exceeded 400 km/s ($K_2 = 409 \pm 18$ km/s). From the radial-velocity curve, Remillard *et al.* [20] determined the system's orbital period ($P_{orb} = 0^d.43325(58)$) and computed the mass function of the compact object, $f(M) = 3.07 \pm 0.40\ M_\odot$. The spectrum of the nova reveals broad Hα and Hβ emission lines, testifying to the presence of an accretion disk around the compact object in the quiescent state. The full widths at half maximum of the Balmer lines reach 1500−2500 Å. Both the line intensities and profiles vary in time, and the line profiles are asymmetric.

In both filters, the system's light curve forms a double wave during the orbital period. The brightness minima coincide with the transitions of the radial velocity of the optical star through the γ velocity, providing evidence for the dominance of ellipsoidal variability of the K star in the optical variations. The I light curve is fairly symmetric, with the variation amplitude being lower than in V ($\Delta I \sim 0^m.15$).

The V light curve is characterized by a higher variability amplitude and appreciably unequal maxima at the quadratures, with the system being brighter at phase $\varphi \sim 0.25$.

Antokhina and Cherepashchuk [21] interpreted the more symmetric I light curve of GU Mus in a standard X-ray binary model with a thin accretion disk around a relativistic object [22], with the disk's radius being ∼0.6 of the maximum size of the Roche lobe of the primary (compact object). They demonstrated that the orbital inclination i showed a weak dependence on the component-mass ratio over a wide range of $q = M_1/M_2$. However, it is not possible to derive a reliable mass ratio for the system solely based on the shape of the infrared light curve. They estimated the lower limit for the orbital inclination $i > 39°$. They also were not able to adequately describe the V light curve's shape and amplitude using this standard model.

Based on observations of GU Mus three years after its outburst, Orosz *et al.* [23] improved the values found in [20] for the system's orbital period ($P_{orb} = 0^d.4326058(31)$), the half-amplitude of the secondary's radial-velocity curve ($K_2 = 406 \pm 7$ km/s), and the compact object's mass function ($f(M) = 3.01 \pm 0.15\ M_\odot$). According to this study, the secondary is a K3−K5 main-sequence star. After subtracting the standard spectrum of a K5V star from the total spectrum, the disk spectrum shows strong Balmer, HeI, and FeII emission lines against a flat continuum. The light-curve modeling of Orosz *et al.* [23] using an ellipsoidal-variability model could not fit the unequal light-curve maxima or the depth of the minimum corresponding to the upper conjunction of the optical star. Based on the absence of eclipses of the disk in the system, Orosz *et al.* [23] estimated the upper limit for the orbital inclination $i_{\max} \sim 65°$. A lower limit was estimated from the minimum amplitude of the V light curve, $i_{\min} \sim 54°$. For the mass ratio $q = M_1/M_2 = 6.5$−8.8, the mass of the primary will be $M_1 \sim 5.0$−$7.5\ M_\odot$.

Casares *et al.* [24] observed the Hα line in the spectrum of GU Mus, confirmed that the secondary has spectral type K3−K4V, and demonstrated that the secondary contributed 85−88% of the integrated R flux. Based on the rotational broadening of the photospheric absorption lines together with the $v \sin i$ value obtained for the secondary with limits based on the system's geometry, they estimated the component-mass ratio to be $q = 7.5$−8.1. They also present Hα Doppler tomography maps revealing a considerable flux from the secondary, probably related to the star's chromospheric activity, with the flux from the hot spot being absent or weak.

Shahbaz *et al.* [25] analyzed the H light curve of GU Mus to derive the orbital inclination $i = 54° \pm 15°$, distance $d \sim 2.8$−4 kpc, and mass of the compact object $M_1 \sim (4$−$11)\ M_\odot$.

Gelino *et al.* [26] acquired infrared light curves of GU Mus in the J and K bands and analyzed their J and K light curves using the code of Wilson and Devinney [27], without taking into account the accretion disk around the compact object or the hot spot. These computations considered only the ellipsoidal variability of the secondary, which was taken to be slightly evolved, since a normal K4V star does not fill its Roche lobe. However, the secondary cannot be a giant: in this case, the star's size would be larger than the orbit corresponding to the orbital period of $0^d.43$. Their analysis of the J and K light curves confirmed the conclusion of Antokhina and Cherepashchuk [21] that the model light curves were fairly insensitive to

input parameters such as the component-mass ratio, the limb darkening and gravitational-darkening coefficients, and the effective surface temperature of the secondary. An exception is the orbital inclination, for which Gelino *et al*. [26] found the best-fit value $i = 52°–56°$. Taking into account additional sources of radiation in the system (the disk and hot spot) increases the admissible orbital inclination by $\sim 4°$. They estimated the mass of the compact object to be $M_1 = 6.95 \pm 0.6\ M_\odot$; the corresponding distance to the system is $d \sim 5.1$ kpc.

3. THE MODEL OF THE SYSTEM

The light curves of GU Mus obtained by various authors show a significant light excess near quadrature, $\varphi \sim 0.25$, which cannot be reproduced in the standard models (phase $\varphi = 0.0$ corresponds to upper conjunction of the compact object). Such models likewise cannot reproduce the deeper minimum at phase $\varphi \sim 0.0$. Heating of the secondary by X-rays from the compact source, which could make the minimum at phase $\varphi \sim 0.5$ shallower, is not strong in this system. For the distance $d \sim 5$ kpc, the X-ray luminosity of the source in its low state does not exceed $L_X < 1.5 \times 10^{32}$ erg/s, but no more accurate value is known. The bolometric luminosity of the optical K3–5V star is $\sim (6–9) \times 10^{32}$ erg/s, so that the ratio of the components' bolometric luminosities is $L_X/L_{\rm opt} \leq 0.2$. The secondary can also receive some fraction of the hot ultraviolet radiation from the inner parts of the disk if this radiation propagates symmetrically. The ultraviolet light could be invisible to an observer on Earth due to absorption in the circumstellar envelope and interstellar medium. However, if the angular distribution of the X-ray flux is not uniform, as is characteristic of black holes [28], the heating of the secondary by this radiation will remain insignificant. In addition, considerable heating of the secondary would lead to variations of the star's spectral type with orbital phase, which are not observed.

To compute the theoretical light curve and derive the X-ray nova's parameters, we used a mathematical model taking into account the contribution of the additional radiation from the shock wave outside the accretion disk. The radiation of this shock is strongest at phase $\varphi \sim 0.25$, but, depending on the conditions for its radiative cooling, it may also be observed at phases $\varphi \sim 0.75$. We successfully used this model earlier in our analysis of light curves of cataclysmic variables [15]. Below, we briefly describe its main features; a more detailed description of the model can be found in [15, 29].

(1) The donor star (secondary) completely fills its Roche lobe.

(2) We take into account the tidal and rotational distortion of the secondary.

(3) The surface of the secondary is subdivided into 648 area elements, and the intensity of the radiation emitted toward the observer is computed for each, taking into account gravitational darkening and limb darkening (applying a nonlinear limb-darkening law). We consider occultations of the area elements on the star by the body of the star itself and by the bodies of all the components of the system. When allowing for the effects of heating of the stellar surface by hot radiation from inner regions of the disk, we use two models, with isotropic and anisotropic angular flux distributions. It was demonstrated in [30] that, for disk accretion onto a neutron star, the star's rotation makes the propagation of radiation from this central source isotropic; i.e., this radiation will not be attenuated in the orbital plane of the system. In the case of a black hole, there is no such central source, and the radiation flux from the flat surface of the accretion disk possesses considerable anisotropy, leading to reduced heating of the companion. However, due to a number of instabilities that accompany high accretion rates [31], the inner parts of the disk can become more spherical, making the radiation from the accretion disk more isotropic. Note that the accretion rates during the quiescent states of X-ray novae are probably low, making it unlikely that the inner parts of the accretion disk become more spherical. The central parts of an advection-dominated disk become spherical due to the high ion temperature [32, 33].

(4) The primary is spherical in shape and is located at a focus of the elliptical accretion disk. Since the compact object is small, we assume when analyzing the light curves of X-ray novae that its optical and infrared luminosities are negligible and do not contribute to the combined flux of the system.

(5) The elliptical (eccentricity e) accretion disk is represented as follows. The lateral (or outer) surface of the disk is an ellipsoid with semi-axes a, b, and c. The semi-axes a and b are in the orbital plane, so that $b^2 = a^2(1 - e^2)$; the semi-axis c is orthogonal to the orbital plane. The center of the primary is at a focus of the ellipsoid.

The disk's orientation is determined by the angle α_e between the radius vector from the center of the compact object to the disk periastron and the line connecting the components of the close binary. The value of α_e can vary from 0 to 2π and increases in the direction of the components' orbital motion. A detailed description of the procedure used to model a thick, elliptical accretion disk was presented in [34].

The temperature of an area element on the disk surface depends on the distance r between its center and the compact object. We assume that the temperature of disk areas near the black hole are equal to the

temperature T_b of the first inner orbit located near the equator at the distance R_1 from its center. Variations of the disk temperature are usually represented by the relation [28]

$$T(r) = T_b \left(\frac{R_1}{r}\right)^{\alpha_g}, \quad (1)$$

assuming that the gravitational energy released during the accretion is balanced by radiative cooling. As a first approximation for the parameter α_g, the value $\alpha_g = 0.75$ [28] is usually used, which corresponds to assuming that each point of the disk's surface emits as a black body. However, observations show that the radial temperature distribution is often flatter than for the canonical case, leading to higher temperatures. Heating of the disk's outer regions by radiation from the secondary increases its temperature only slightly, but the model also takes this into account. The outer boundaries of the disk can also be heated by high-temperature radiation from its inner regions. This effect is significant only when this radiation propagates isotropically; in this case, it also heats the secondary. If high-temperature radiation with luminosity L_b from the inner regions of a classical accretion disk propagates anisotropically, the flux L reaching the surface of the secondary varies according to the relation [30]

$$\frac{dL}{d\Omega} = \frac{L_b \cos\theta(1 + u_b \cos\theta)}{2\pi\left(1 + \frac{2}{3}u_b\right)}. \quad (2)$$

Here, the limb darkening in the accretion disk has been included in a linear approximation, θ is the angle between the normal to the disk's surface and the direction of the solid-angle element $d\Omega$, and u_b is the limb-darkening coefficient of the disk. For the case of isotropic flux propagation, this simplifies to

$$\frac{dL}{d\Omega} = \frac{L_b}{4\pi}. \quad (3)$$

(6) The hot line along the flow is described using part of an ellipsoid with semi-axes a_v, b_v, and c_v elongated toward the inner Lagrangian point, L_1. The lateral surface of this ellipsoid coincides with the tangent to the elliptical disk for all disk orientations, and its center is in the orbital plane in the disk, at some distance from its edge. Only that part of the ellipsoid outside the accretion disk is considered to be the hot line. The procedure used to construct the shape of the hot line and the technique used to synthesize the light curve of a close binary in the framework of the model used are described in [29].

The release of the shock energy occurs at the surface of the hot line, both at the shock front (i.e., on the side of the approaching flow, or the "windward side") and on the opposite ("leeward") side, depending on the physical parameters of the interacting flows (their velocities, densities, etc.). Areas on the surface of the hot line are assumed to radiate according to a Planck law, which means the hot line adjacent to the accretion disk is considerably opaque. We compute the temperature of an area element on the surface of the hot line independently for both its sides, in accordance with the relation

$$T_i(y) = T_d + T_0 \cos(0.5\pi\Delta y_i), \quad (4)$$
$$\Delta y_i = \frac{y_i - y_{\max}}{y_{\min} - y_{\max}},$$

where T_d is the temperature matter would have at the distance r from the compact object according to Eq. (1). At the point with the coordinate $y_{\max}$, the temperature of the matter in the hot line, $T_i(y)$, has the largest increment, $T_{\max}(y) = T_d + T_0$, and, at the point with $y_{\min}$, the temperature increment is equal to zero, and the temperature of the matter is $T_i(y) = T_d$. When $y_{\min}$ and $y_{\max}$ are close to each other, the energy release from the shock occurs in a small region resembling a hot spot, but located not on the disk but instead on one part of the hot-line surface, with its other parts remaining comparatively cool. It is assumed that the temperature on the windward side of the hot line reaches its highest value, $T_{\max}$, at the point of contact between the flow and the lateral surface of the disk. The highest temperature of the hot line on the leeward side is displaced to the point with

$$y^{(2)}_{\max} = y^{(1)}_{\max} - dy,$$

with the displacement dy being a free parameter of the problem, $dy > 0$. Here, the superscripts (1) and (2) refer to the windward and leeward sides of the hot line, respectively.

The model parameters we wish to estimate are $q = M_1/M_2$, i, T_2, and T_b; the disk eccentricity e and semi-major axis a; the parameter α_g determining the profile of the temperature variations across the disk surface; the azimuth of the disk's periastron α_e; the parameter A_p determining the thickness of the disk's outer edge; the semi-axes of the ellipsoid describing the ellipsoidal part of the hot line a_v, b_v, and c_v; the highest temperatures on the surface of the hot line near the outer edge of the disk at its windward side, $T^{(1)}$, and leeward side, $T^{(2)}$; and the parameters $y_{\min}$ and dy described above. Thus, there are a total of 16 parameters; however, we were able to fix some of these (cf. Section 4).

(7) We searched for the parameters best describing the system's mean light curve using the Nelder–Mead method [35]. When searching for the global minimum of the residual for each of the curves, we applied several dozen different first approximations, due to the large number of independent variables,

which typically leads to the existence of a number of local minima in the studied parameter range. We estimated the quality of the fit between the theoretical and observed light curves using the residual

$$\chi^2 = \sum_{j=1}^{n} \frac{(m_j^{theor} - m_j^{obs})^2}{\sigma_j^2}, \qquad (5)$$

where m_j^{theor} and m_j^{obs} are the object's theoretical and observed magnitudes at the jth orbital phase, σ_j^2 is the dispersion of the observations for the jth data point, and n is the number of normal points in the curve.

4. RESULTS OF LIGHT-CURVE MODELING FOR GU Mus

We determined the parameters of GU Mus using two models. The first assumed isotropic propagation of the X-ray and high-temperature ultraviolet radiation from inner parts of the disk. In the second, we allowed for angular anisotropy of the propagation of this radiation.

As noted in Section 3, the reason for the anisotropy of the X-ray radiation from the inner parts of a classical accretion disk is that, in the case of a black hole, the flat inner part of the disk radiates similarly to a thin stellar atmosphere. In this case, the radiation intensity is highest along the normal to the surface and decreases rapidly with deviation from the normal direction. In addition, due to the effect of projection, the radiating area of the flat disk surface also decreases with deviation from the normal direction. According to [28], this leads to a strong angular dependence for the X-ray intensities of accreting black holes [cf. Eq. (2)].

Light curves used. We used three groups of light curves of GU Mus to determine its parameters. The first consists of light curves acquired in white light (effective wavelength $\lambda \sim 5000$ Å) in 1992–1995 (designated BV, cf. Figs. 1, 2), and the second group are I curves ($\lambda_{eff} = 9000$ Å) acquired in 1992 and 1993. The BV and I observations are presented graphically in [23]. The 1992 light curves for BV and I are also described in detail by Remillard *et al.* [20]. The mean BV and I light curves are shown in Figs. 1–3. All these observations correspond to the system's low state, but comparison of the mean fluxes shows that GU Mus was $\sim 0^m.2$ brighter during 1993–1994 than in 1992 or 1995. The light-curve shape varies from season to season; the relative height of the brightness maxima at the quadratures in 1993–1995 was opposite to that observed in 1992. Both the absolute and relative depths of the brightness minima vary in both filters. We can see that the modulation amplitude and the difference between the maxima of the light curve at the quadratures increase with decreasing wavelength, especially for the 1992 season. The phase $\varphi = 0.0$ corresponds to the upper conjunction of the compact source. The I light curves are more symmetric due to the lower contribution of the accretion disk and possibly of the shock, since the optical star is, on average, cooler than the disk.

The third group of light curves we used are the J, K light curves of GU Mus presented by Gelino *et al.* [26], which were also acquired during the system's low state, on February 20 and 21, 2000.

The number of normal points n used to fit the shape of the mean BV, I, J, and K light curves of GU Mus are presented in the table, along with the corresponding critical $\chi^2_{0.01,n}$ values for the $\alpha = 0.01$ significance level; thus, the probability that the actual parameters of the system are outside the ranges derived from our light-curve analysis does not exceed 1%. Since the nature of the X-ray and ultraviolet heating of the optical star remains unclear, we analyzed the light curves independently for the cases of isotropic and anisotropic radiation from the inner regions of the accretion disk.

Optical light curves of 1992–1995. When constructing the theoretical light curves, we computed the radiation fluxes from the system's components, $F(X, \varphi)$, for a given set of parameters X and a sequence of orbital phases, φ. The resulting $F(X, \varphi)$ values are expressed in relative units. These can be converted into commonly used units (referring to a unit wavelength interval) using the expression $f = Fa_0^2 \times 10^{-12}$ [erg s^{-1} cm^{-3}], where a_0 is the distance between the centers of mass of the stars in centimeters. When interpreting individual light curves, during the construction of a trial theoretical curve, we usually used the flux at the first quadrature corresponding to the given trial curve to convert the computed radiation fluxes to magnitudes. For comparison with the observed light curve, we initially shift the computed trial light curve to achieve the best agreement between the observed and computed radiation fluxes (in magnitudes) at the first quadrature. The subsequent comparison of the observed and synthesized light curves uses the χ^2 criterion.

Since the number of model variables could be as high as 16, it is necessary to use additional information to choose the most probable solutions from the large number of sets of admissible parameters obtained from the light-curve fitting. This includes spectroscopic information about the mass ratio of the close-binary components, as well as data on the red dwarf's contribution to the combined radiation flux during the studied observing period. Information on the red dwarf's contribution to the combined flux is

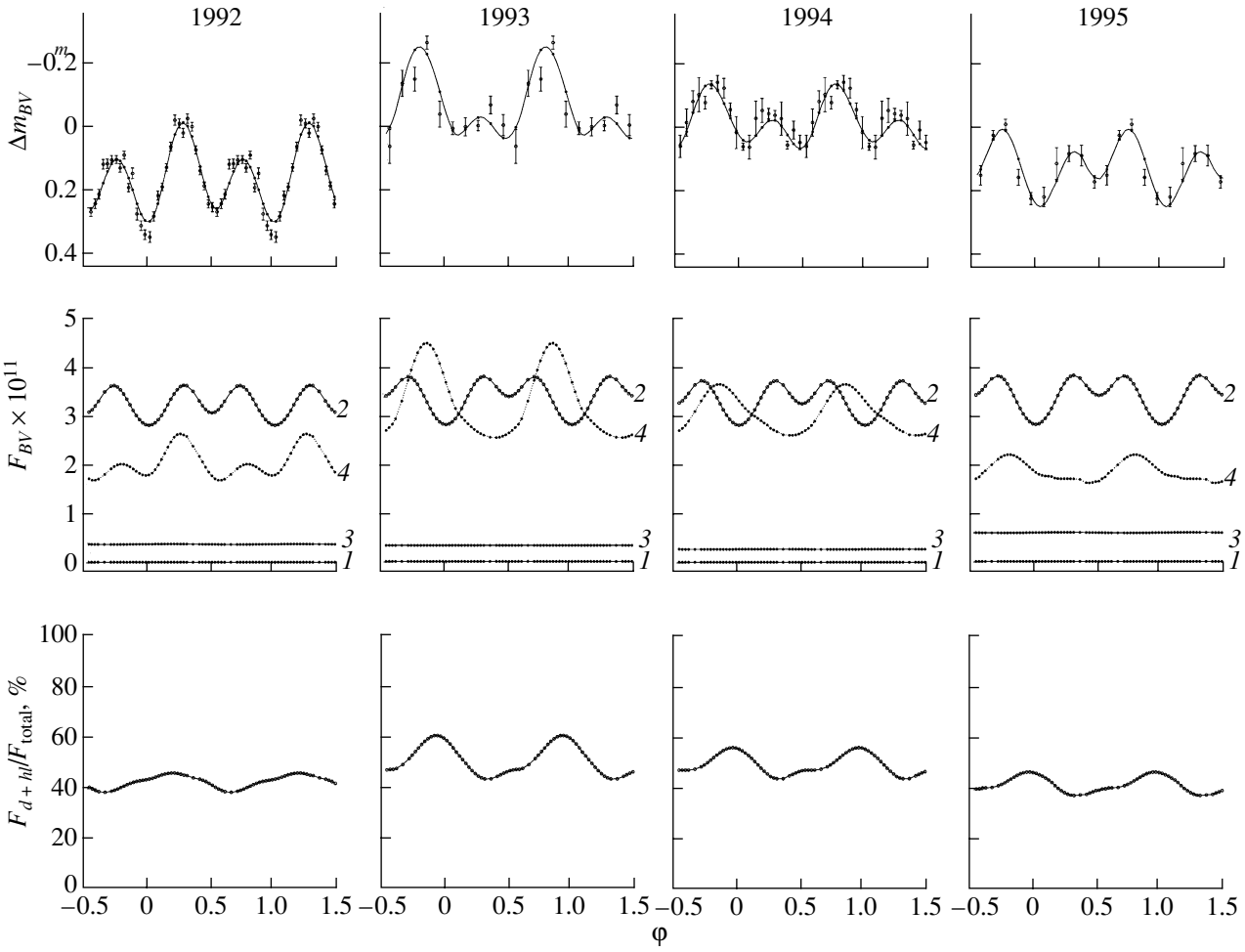

Fig. 1. Computational results for the model with isotropic radiation from the inner parts of the accretion disk. The upper panels show 1992–1995 observations of GU Mus in the optical ($\lambda = 5000$ Å; points with corresponding error bars) and theoretical curves (solid) computed using the parameters given in the table. The middle panels show the contributions of the (*1*) compact object (equal to zero in both models), (*2*) red dwarf, (*3*) elliptical accretion disk, and (*4*) extended hot line to the combined flux. The bottom panels show the relative contribution of the nonstellar radiation sources (disk and hot line) to the combined flux from the system.

very limited. According to the spectroscopic observations of Orosz *et al.* [23] obtained in 1993, the contribution of the secondary to the combined BV flux was 46–48%, with the corresponding contribution of the nonstellar sources of radiation being 52–54%. The luminosity of GU Mus was lower in 1992 due to the decreased flux from the nonstellar components; as a result, the relative contribution of the red dwarf's light to the total flux increased to 55–61%. This estimate of the contribution of the optical star to the combined flux was obtained using the standard approach: the equivalent widths of the stellar absorption lines for the binary were compared to the equivalent widths of the absorption lines in the spectrum of a standard star, which is a single star of a similar spectral type and luminosity class.

When searching for the parameters of the GU Mus components for different observing seasons, we expressed all four observed BV light curves ($\lambda_{eff} \sim 5000$ Å) in magnitude differences, Δm_{BV}, relative to the system's magnitude at phase $\varphi = 0.25$ ($m_{BV} = 20^m.3684$) for the 1993 light curve (this light curve's number is $N = 2$):

$$\Delta m = m_N^{obs}(\varphi) - m_2^{obs}(\varphi) = -2.5 \log \left(\frac{F_N^{obs}(\varphi)}{F_2^{obs}(0.25)} \right).$$

In other words, this flux, in magnitudes, was used as a unified energy unit for all other observed light curves. Thus, all the 1992–1995 observations were reduced to the same zero point, corresponding to the observed flux at the first quadrature of the 1993 light curve. This approach enabled us to estimate variations of the system's luminosity from one light curve to another for each phase and to use both the light-curve shape

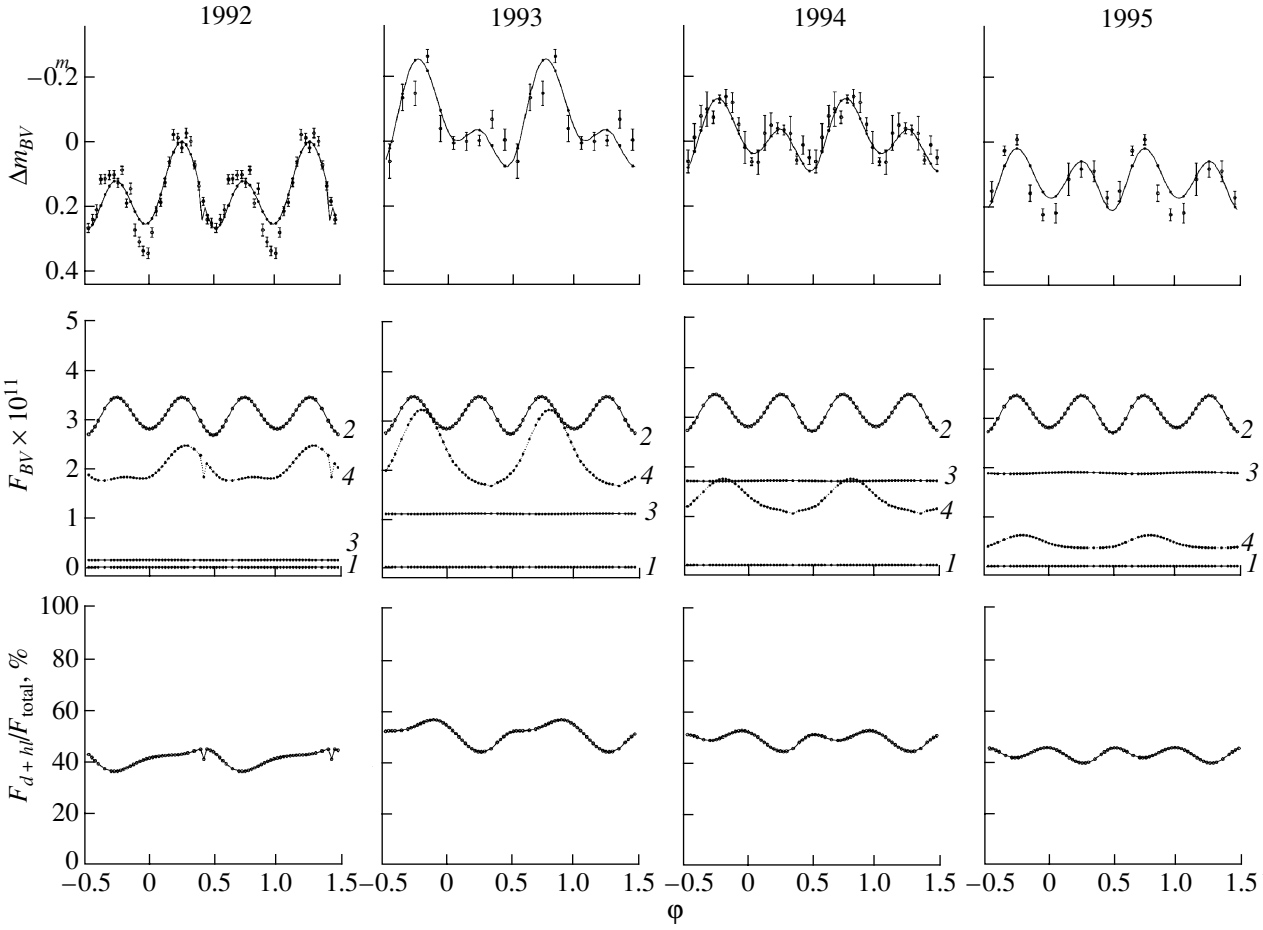

Fig. 2. Same as Fig. 1 for the model with anisotropic radiation from the inner parts of the accretion disk.

(as in the analysis of the individual light curves) and changes of the mean flux levels when comparing with the synthesized curves.

Thus, we constructed the Nth trial theoretical light curve in magnitudes by converting the theoretical fluxes, $F_N^{th}(X,\varphi)$, computed in the model into magnitudes, $\Delta m_N^{th}(X,\varphi)$, using the flux at the first quadrature for the same theoretical curve that best fitted the observed light curve with $N=2$, $F_2^{th}(0.25)$. In other words, the theoretical magnitude at phase φ for the Nth light curve will be

$$\Delta m_N^{th}(\varphi) = -2.5\log\left(\frac{F_N^{th}(\varphi)}{F_2^{th}(0.25)}\right).$$

The number of unknown parameters was largest in the first stage of solving for the parameters of GU Mus using each of the studied BV light curves. In the second stage of the analysis, we found the values of q, i, T_2 common to all the curves (close to the mean values). These parameters can be best determined from the J,K observations, because the star's optical light makes the highest contribution in these filters, but the normal points of the J,K light curves [26] have very high uncertainties, leading to a large range of admissible values for q and i. Therefore, when selecting the optimal q, i, T_2 values to fix, we used the parameters derived from the infrared light curves using the same weight as for the parameters derived from the BV light curves. We also fixed common values close to the mean parameter estimates for the disk's maximum radius (at apoastron), R_d/ξ (ξ is the distance between the center of mass of the compact object and the inner Lagrangian point, L_1), the thickness of the disk's outer edge β_d, the parameter α_g determining the radial temperature distribution in the disk, and the inner radius of the disk R_1 [this last parameter is needed to derive the radial temperature distribution of the disk; cf. (1)]. We then repeated the fit for the system's parameters for all four light curves fixing the parameter values $q = M_1/M_2 = 7.7$ (close to the spectroscopic estimate), $i = 54°$, $T_2 = 4500$ K, $R_1 = 0.0006a_0$, $R_d/\xi = 0.50$, $\beta_d = 1\overset{\circ}{.}8$, and $\alpha_g = 0.72$ for both the isotropic and anisotropic models.

Since we fixed the parameters of the secondary

Parameters of the components of GU Mus in 1992–2000, derived from the BV, I, J, K light curves in the hot-line model

Parameter	1992	1993	1994	1995	1992	1993	2000	2000
				"Isotropic" model				
n	30	10	20	10	25	10	29	22
$\chi^2_{0.01,n}$	50.9	23.2	37.6	23.2	44.3	23.2	49.6	40.3
Filter	BV				I		J	K
e	0.395	0.043	0.074	0.270	0.001	0.033	0.174	0.043
a/a_0	0.250	0.334	0.324	0.274	0.348	0.337	0.297	0.334
α_e, °	113.8	63.2	72.3	97.2	140.6	84.7	112.6	33.9
T_b, K	115255	133650	127340	134070	114800	132300	96935	97650
a_v/a_0	0.054	0.098	0.093	0.058	0.104	0.148	0.075	0.079
b_v/a_0	0.582	0.362	0.324	0.530	0.325	0.307	0.422	0.442
c_v/a_0	0.017	0.011	0.010	0.005	0.007	0.018	0.010	0.019
$T_{1*(\max)}$	10480	54850	15300	13210	6460	26505	15880	29670
$T_{2*(\max)}$	8500	30170	8985	11570	3195	14100	8150	12895
$\langle T_1 \rangle$	3620	2100	6480	2950	4565	5130	5245	19580
$\langle T_2 \rangle$	3070	2200	5630	2920	2065	4665	3515	9555
$y_{\min}/a_0$	0.321	0.236	0.273	0.248	0.367	0.276	0.291	0.411
$y_{\max}/a_0$	0.198	0.232	0.213	0.170	0.203	0.262	0.196	0.215
dy/a_0	0.261	0.0	0.097	0.251	0.217	0.015	0.151	0.014
χ^2	103	22.1	33.3	10.3	70.5	17.5	37.7	10.6
				"Anisotropic" model				
e	0.336	0.141	0.123	0.267	0.000	0.214	0.287	0.059
a/a_0	0.261	0.305	0.310	0.275	0.348	0.287	0.271	0.328
α_e, °	157.9	92.9	92.4	110.8	138.4	175.0	131.3	83.3
T_b, K	101425	158865	175055	170155	75340	147730	85010	90320
a_v/a_0	0.046	0.077	0.073	0.058	0.013	0.063	0.046	0.076
b_v/a_0	0.558	0.343	0.381	0.432	0.518	0.401	0.575	0.448
c_v/a_0	0.007	0.006	0.006	0.006	0.006	0.006	0.010	0.019
$T_{1*(\max)}$	15765	18785	14600	8515	19885	11600	11935	32725
$T_{2*(\max)}$	9475	11530	94845	8380	2030	8370	8630	11782
$\langle T_1 \rangle$	3010	3730	3395	2985	1410	2480	3035	18065
$\langle T_2 \rangle$	2345	5275	3935	3135	1055	2445	2630	7985
$y_{\min}/a_0$	0.24	0.25	0.25	0.26	0.13	0.21	0.29	0.38
$y_{\max}/a_0$	0.20	0.20	0.19	0.17	0.12	0.18	0.18	0.21
dy/a_0	0.226	0.129	0.178	0.297	0.358	0.238	0.188	0.032
χ^2	222	33.9	34.6	45.3	153	29.8	40.7	10.8

Note. Solutions were found for the cases of isotropic and anisotropic propagation of the radiation from the inner parts of the accretion disk with temperature T_b. The following parameters were fixed: $q = 7.70$, $i = 54°$, $T_2 = 4500$ K, $R_1 = 0.0006a_0$, $R_2 = 0.230a_0$, $R_d/\xi = 0.50$, $\beta_d = 1{}^{\circ}\!.8$, and $\alpha_g = 0.72$. $\chi^2_{0.01,n}$ is the critical χ^2 value for the $\alpha = 0.01$ significance level, and n is the number of normal points in the mean light curves of GU Mus.

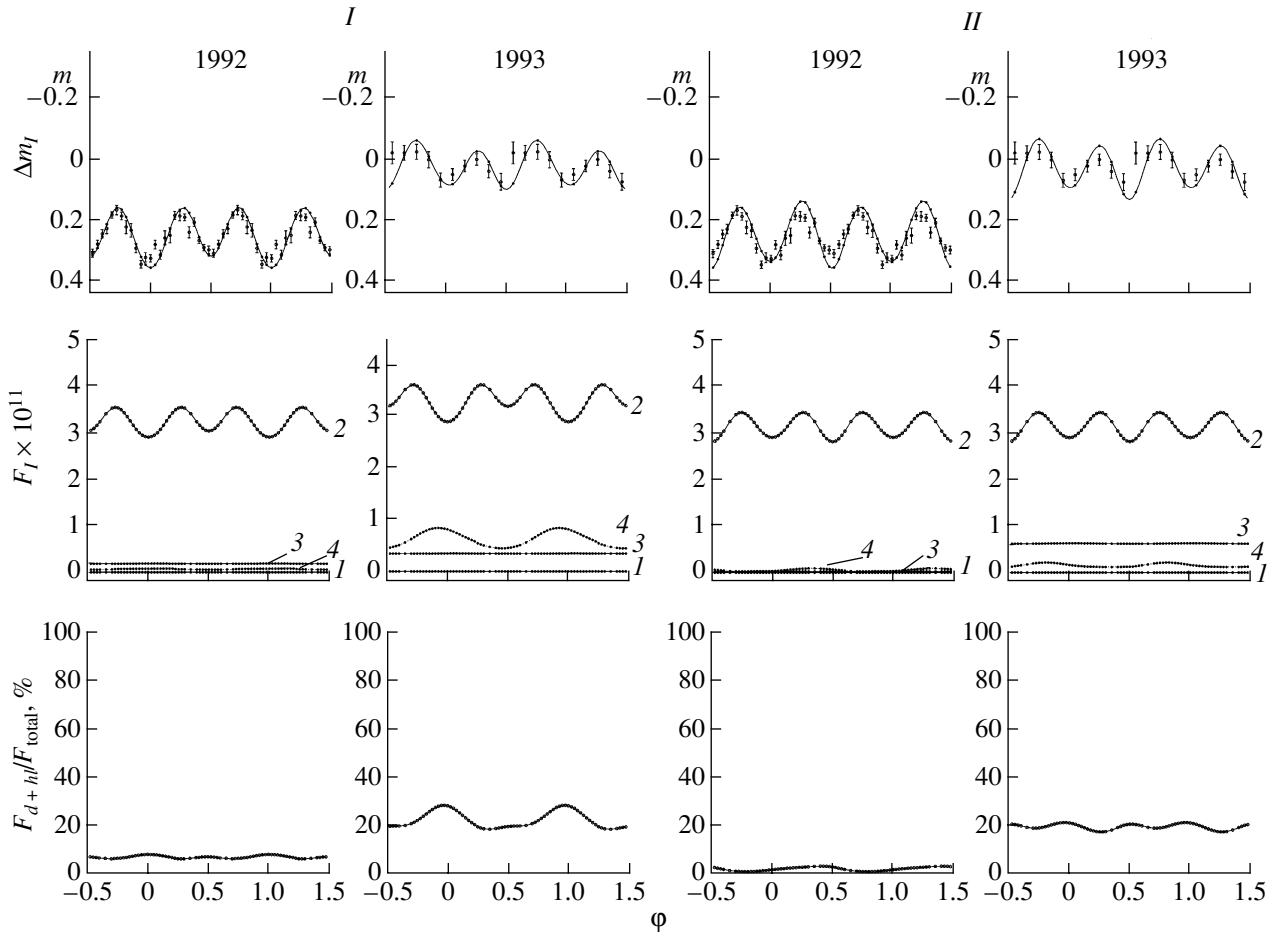

Fig. 3. Computational results for the models with isotropic (I) and anisotropic (II) radiation from the inner parts of the accretion disk derived from near-infrared (I) observations of GU Mus. The upper panels show the 1992–1993 observations (points with corresponding error bars) and theoretical curves (solid) computed using the parameters given in the table. The notation is the same as in Fig. 1.

in the computations, the contribution of its light to the combined flux depends only weakly on the trial set of remaining parameters (slight variations were found only at phase $\varphi = 0.5$, during the secondary minimum, due to re-radiation of the ultraviolet flux from inner parts of the disk by the body of the star in the case of isotropic propagation of the initial radiation). As a result, variations of the flux of the system are mainly determined by variations in the contributions of the nonstellar components of the close binary. We determined the best-fit parameters for the 1993 light curve based on the set of X_i values that gave the smallest residuals, for which the mean contribution of the light from the disk and hot line averaged over an orbit was 52–54%, in agreement with the spectrophotometric estimate [23] for that epoch. We accordingly used this value of the theoretical flux, $F_2^{th}(0.25)$, to calculate the theoretical 1992–1995 light curves in magnitudes when translating the theoretical fluxes, $F_N^{th}(X, \varphi)$, into magnitudes, $\Delta m_N^{th}(X, \varphi)$.

The table contains the parameters of the disk and hot line for 1992–1995, computed for the cases of isotropic and anisotropic propagation of the high-temperature ultraviolet radiation and X-rays from the inner parts of the disk. In the upper part of the table, we indicate the numbers of normal points for each of the light curves and their corresponding critical χ^2 values for the $\alpha = 0.01$ significance level. We can see that the agreement between the theoretical and observed light curves is somewhat better for the isotropic model. The solid curves in the upper panels of Fig. 1 are the theoretical curves for the 1992–1995 observations computed using the parameters from the table.

The hot-line model obtained assuming isotropic propagation of the radiation from the inner parts of the disk provides a very good fit to the observations of

the X-ray nova GU Mus, for both the standard 1993–1995 light curves with the normal luminosity ratio at the quadratures and the 1992 BV light curve with its anomalous distribution of the radiation fluxes at the quadratures. This can be achieved by increasing the contribution of the visible light from the hot line at phases ~ 0.25, due to the increase in the length of the shock along the line and the more favorable orientation of the disk and line for that epoch (see below).

There is a significant contribution to the secondary's brightness in the isotropic model due to the reflection effect, i.e., from reprocessing of the high-temperature radiation (X-rays and ultraviolet light) from inner parts of the disk in the atmosphere of the red dwarf. Such heating is strongest in the hemisphere facing the compact source (with the exception of equatorial regions of the star, due to screening by the disk itself). As a result, the minimum at phase $\varphi \sim 0.5$ is shallower than when the heating is not taken into account, and the minimum at phase $\varphi \sim 0.0$ is deeper [compare Figs. 1 and 2, where we show the contributions of the optical star to the combined flux (*2*) for the cases of a considerable reflection effect (Fig. 1) and virtually no reflection effect (Fig. 2)].

The middle panels of Fig. 1 show the contributions of the light from the system's components to the combined flux. In the isotropic model, the contribution of the disk varied little from epoch to epoch. The influence of the hot-line flux and its variations in the course of the system's orbital motion is much stronger. In particular, the anomalous shape of the light curve in 1992 is due to a significant increase of the flux from the windward side of the line (seen at phases $\varphi \sim 0.25$) compared to the flux from the leeward side ($\varphi \sim 0.75$). The hot-line flux depends on the size of the emitting region and the temperature at the shock front. We can estimate the size of the emitting region on the surface of the hot line from $y_{\max}$ and $y_{\min}$ (see the table), which are the y coordinates of the areas along the axis of the hot line on the windward side with the highest and lowest temperatures (recall that the highest temperature on the windward side of the line, $T_{\max}^{(1)}$, is reached where the hot line intersects the disk, whereas the leeward-side region with the highest temperature, $T_{\max}^{(2)}$, is displaced along the y axis by $dy = y_{\max}^{(1)} - y_{\max}^{(2)}$, where the superscripts 1 and 2 refer to the windward and leeward sides of the hot line). We can see from the table that the size of the hot region on the windward side of the line was quite large in 1992 ($\Delta y \sim 0.123 a_0$). The size of the emitting region on the leeward side (at phases $\varphi \sim 0.75$) is almost twice that on the windward side, and the ratio of the hot-line fluxes at phases $\varphi \sim 0.25$ and ~ 0.75 depends strongly on how much higher the mean temperature of the line material is on the windward side than on the leeward side.

Another important factor is the possible occultation of the brightest region of the shock by the edge of the disk. For the 1992 light curve, the mean temperature of the hot line on the windward side turned out to be almost 15% higher than on the leeward side. The combination of the large size of the hot-line emitting region and the temperature ratio was significant in making the radiation flux from the windward side higher than that from the leeward side. Figure 3 (column *I*) schematically displays the components of GU Mus in the optical. The shading shows emitting regions on the surface of the hot line for different years.

The length of the optically thick hot line in 1995 was approximately the same as in 1992, but the linear size of the emitting region was half as large ($\Delta y \sim 0.078 a_0$); the mean hot-line temperatures coincided within the errors. As a result, the luminosity from the leeward side of the hot line was higher than that from the windward side, and the variations of the radiation flux from this component were similar to those expected for hot-spot models. We see a similar picture for the 1993–1994 light curves. The hot line was quite short and resembled a modest bulge on the disk, and the linear size of the emitting region was even smaller ($\Delta y \sim 0.004 a_0$ and $\sim 0.060 a_0$ for 1993 and 1994, respectively). The main flux comes from the leeward side of the line. The increase in the hot-line luminosity in 1993 was due to a considerable increase in its highest temperature, to $\sim 30\,000$ K on the leeward side, though the mean brightness temperature for the entire surface of the hot line was not high due to the small size of the emitting region with the highest temperature. In 1994, the highest hot-line temperature decreased almost threefold. However, due to the increased linear size of the emitting region, the maximum flux from the line was reduced by only 20%.

The bottom panels of Fig. 1 present the relative contributions of the nonstellar radiation sources to the combined flux. The contribution of the secondary's light remained practically constant during 1992–1995. Thus, in this period, the main origin of variations of the system's flux were changes in the luminosities of the disk and hot line. The contribution of the nonstellar components to the combined luminosity of the system estimated using the 1992 light curve is $\sim 42\%$, in good agreement with the spectrophotometric estimate of [23], 39–45%.

With the anisotropic model for the propagation of radiation from the inner parts of the disk, the agreement between the observed and theoretical curves

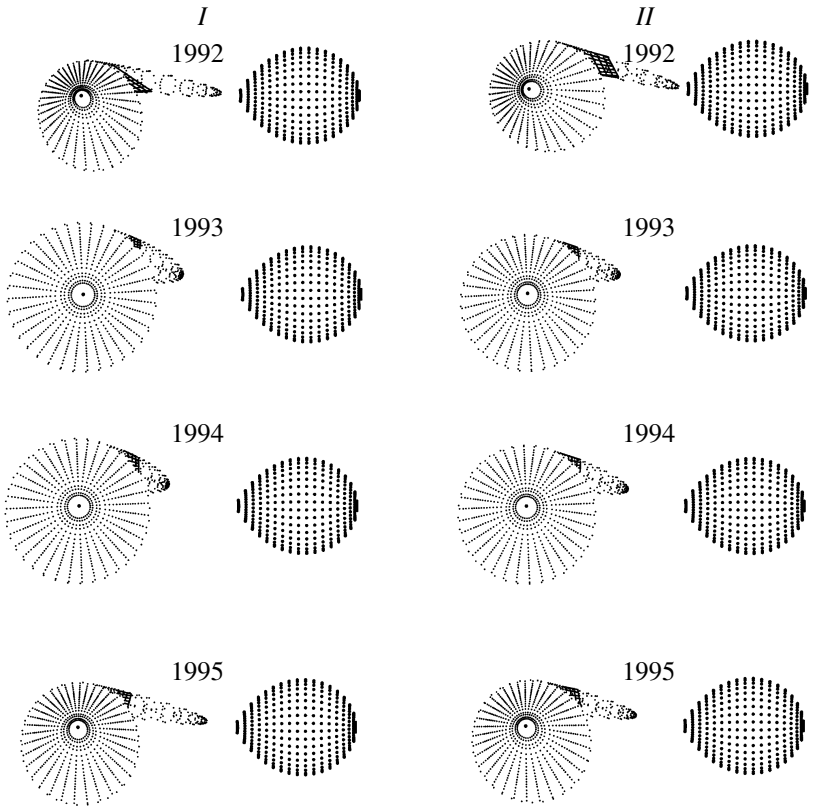

Fig. 4. Schematic of the components of GU Mus during the 1992–1995 observations for the models with isotropic (I) and anisotropic (II) radiation from the inner parts of the disk. The shading shows the emitting regions on the surface of the hot line in different years.

becomes worse for all four light curves (cf. the bottom part of the table). For example, in 1992, the anisotropic model predicted higher fluxes in the primary minimum and, correspondingly, a poorer agreement with the observations.

Comparison of the BV light curves of GU Mus obtained in 1993–1995 shows that it is very difficult to describe the rather shallow minimum of the observed light curves at phase $\varphi = 0.5$ in the anisotropic model. The theoretical flux is lower at phase $\varphi \sim 0.5$ than at phase $\varphi \sim 0.0$. Due to the angular distribution of the hot radiation from inner parts of the disk in the anisotropic model, the reflection effect is negligible, and variations of secondary's flux are determined solely by effect of its ellipticity, which are known to give rise to two minima with equal amplitudes, at photometric phases 0.25 and 0.75, and a deeper minimum at phase $\varphi \sim 0.5$ due to the star's gravitational darkening near the inner Lagrangian point L_1, which is most visible at such phases.

The solid curves in the upper panels of Fig. 2 are the theoretical curves for the 1992–1995 observations for the anisotropic model with the parameters from the table. The luminosity of the hot line in the anisotropic model for 1992–1995 (cf. the model parameters in the table) experienced variations similar to those for the isotropic model. In this case, the luminosity of the disk needed to reproduce the observed flux from the system is much higher than in the isotropic model. Schematic images of the components of GU Mus in the optical obtained for the anisotropic model for 1992–1995 are shown on the right-hand side of Fig. 4 (column II).

Thus, the isotropic-radiation model is better able to fit the shape of the BV light curves for the low-mass X-ray binary GU Mus. Our analysis of the optical BV light curves indicates that, in the GU Mus system during quiescence, there exists a source of ultraviolet light in the central parts of the accretion disk whose luminosity is higher than the X-ray luminosity, L_X, giving rise to a significant reflection effect from the optical star. The origin of this ultraviolet light remains unclear, as does the origin of the X-rays in the low state of the system.

I light curves of 1992–1993. The shapes of both the 1992–1993 I light curves of GU Mus are close to the standard one, with the system's brightness lower at the first than at the second quadrature (Fig. 3). The curves are symmetric, but the deeper minimum is at

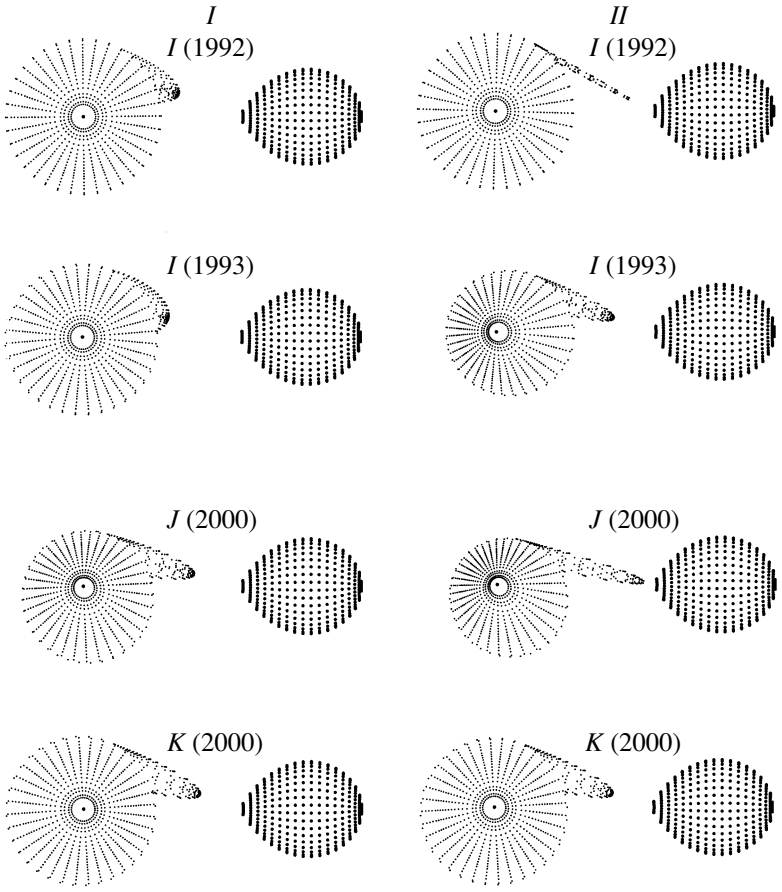

Fig. 5. Schematic of the components of GU Mus for the observations of 1992–1993 (I band) and 2000 (J and K bands) for the models with isotropic (I) and anisotropic (II) radiation from the inner parts of the disk.

phase $\varphi \sim 0.0$ rather than phase 0.5, so that non-ellipsoidal variations also contribute to the I light curve. The higher brightness at phase 0.5 testifies to the presence of an additional source of light, usually believed to be due to heating of the red dwarf by radiation from its companion. The higher brightness of the system at phase 0.75 is sometimes attributed to the emission of a hot spot at the outer edge of the disk.

The I light curves of GU Mus were analyzed using a model with purely ellipsoidal variability in [21, 23]. Both the BV and I observations were reduced to standard magnitudes by Orosz *et al.* [23], taking into account interstellar reddening using the value $E(B-V) = 0^m.29$ derived by Cheng *et al.*. Both studies [21, 23] assumed that the contribution of nonstellar sources of additional light to the system's light curve was small and did not vary with the system's orbital motion. We used our hot-line model to interpret the I light curves of Orosz *et al.* [23]. The resulting parameters for the GU Mus system in 1992 and 1993 are in good agreement with the values found for the system's optical radiation during the same time intervals (see the table).

Only Casares *et al.* [24] have estimated the contribution of light from nonstellar sources in the infrared. Their observations indicate that the contribution of the secondary to the R flux from the system is 85–88%. No similar estimates are available for spectral bands further in the infrared. The bottom panels of Fig. 3 show the relative contributions of the light from the disk and hot line to the combined flux derived by fitting the 1992 and 1993 I light curves using the isotropic (I) and anisotropic (II) models. This contribution was 5–7% in 1992 but increased to 20–25% in 1993. Due to the low contribution of the light of the disk and hot line to the combined flux in 1992 and its insignificant variability in the course of the orbital motion, the 1992 I light curve corresponded best to the model with purely ellipsoidal variability. The assumption of isotropic heating of the stellar surface by radiation from inner parts of the disk whose material is heated to the effective temperature T_b leads to consistent effective temperatures for BV and I light curves ($T_b = 115\,000 \pm 200$ K).

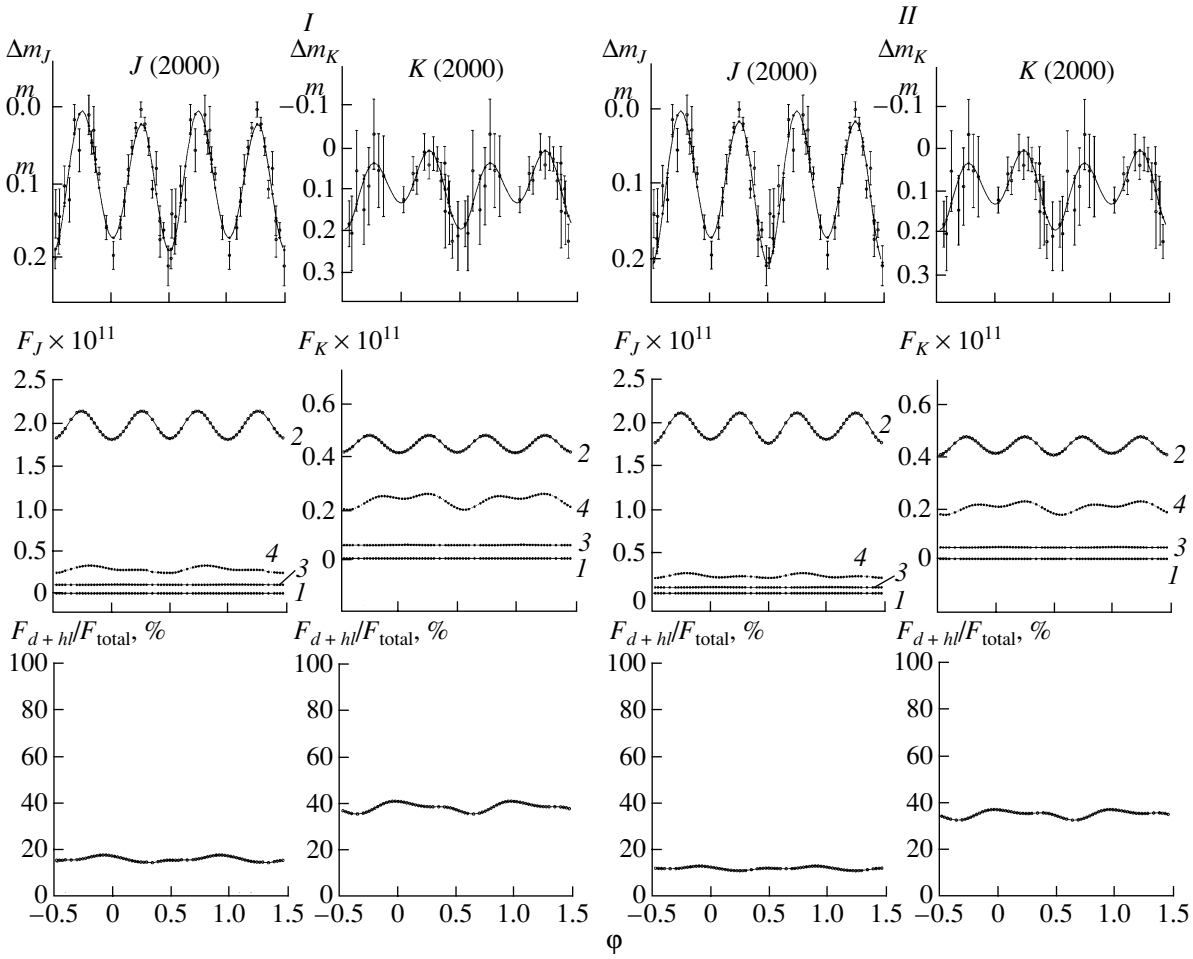

Fig. 6. Computational results for the models with isotropic (I) and anisotropic (II) radiation from the inner parts of the accretion disk obtained for the observations in the far infrared (J and K). The upper panels show the observations of GU Mus for 2000 (points with corresponding error bars) and the theoretical curves (solid) synthesized using the parameters given in the table. The notation is the same as in Fig. 1.

The table contains the parameters of the system derived from the 1992 and 1993 I light curves of GU Mus in both models, and the upper panels of Fig. 4 display the theoretical light curves computed using these parameters. The lowest residual for the 1992 light curve ($\chi^2 = 70.5$) is above the critical χ^2 value for the 1% significance level ($\chi^2_{0.01,25} = 44.3$), even in the isotropic model, despite the good reproduction of the light-curve shape. The reason is that the normal points of the 1992 I light curve demonstrate appreciable scatter, whereas the observing errors, σ_i, are comparatively low, probably testifying to physical variability of the system. The 1993 curve is well described by the isotropic model ($\chi^2 = 17.5$, while the critical χ^2 residual for the 1% significance level is $\chi^2_{0.01,10} = 23.2$).

The middle panels of Fig. 4 show the contributions of the system's components to the combined flux. Compared to 1992, the 1993 infrared fluxes for both the disk and hot line increased, by factors of about two and of more than ten, respectively, giving rise to an increase of the system's overall brightness, a stronger reflection effect, and the appearance of signatures of an orbital hump in the light curve (the observed flux from the system is higher at phase $\varphi \sim 0.75$ than at phase 0.25). At that time, the hot line was transformed into a small bulge on the outer surface of the disk (Fig. 5).

The discrepancy between the T_b values derived from the optical and infrared light curves using the anisotropic model exceeds the errors: $T_b \sim 100\,000$ and $T_b \sim 75\,000$ K, respectively. The agreement between the I observations and the theoretical light curves is a factor of two better for the isotropic than for the anisotropic model, which is not able to reproduce the depth of the secondary minimum of the I light curve without taking into account the reflection effect. Thus, even the 1993 light curve, which is fit

well by the isotropic model, is fit much worse by the anisotropic model ($\chi^2 = 29.8$, whereas the critical χ^2 value for the 1% significance level is $\chi^2_{0.01,10} = 23.2$).

J and K light curves for 2000. We interpreted the J, K light curves of GU Mus acquired by Gelino *et al.* [26] using the same technique we applied to the homogeneous BV and I light curves of [23]: the observed J, K light curves were reduced to the corresponding fluxes at the first quadrature ($m_J = 18.04$, $m_K = 16.97$).

The upper panels of Fig. 6 display the theoretical J, K light curves for the parameters providing the lowest residual, estimated fixing the parameters of both the stars and applying the above restrictions on the fluxes from the nonstellar components (see the table). When the temperature of the inner parts of the disk is $\sim$90 000 K, the reflection effect is negligible at these wavelengths, and the isotropic (I) and anisotropic (II) models give similar results. The residuals for both models are below the critical significance level, and neither model can be rejected on the basis of this criterion. The middle panels of Fig. 6 show the contributions of the light from the system's components in the J and K filters for both models, while the lower panels illustrate the relative contributions of the light from the nonstellar components to the combined flux. In the J filter, this contribution is $\sim$13–17% for the isotropic and $\sim$11–14% for the anisotropic model, close to the estimates presented by Casares *et al.* [24] derived from spectrophotometric R observations, $\sim$12–15%. For the chosen parameters, the contribution of the light from the disk and shock in the K filter increases to $\sim$35%, on average: the flux from the hot line is comparable in both filters, while the K flux from the red dwarf is a factor of four to five lower than in the J filter. Since the fraction of light from the hot line increases in the K filter due to the contribution of free–free radiation in the infrared, to obtain the hot-line flux required to fit the shape of the K light curve, its brightness temperature must be a factor of $\sim$1.5–2 higher than its value in the J band. This conclusion is in agreement with the estimates of the contribution to the infrared flux from free–free transitions in the disk and hot-line material obtained for other cataclysmic variables [15].

Our self-consistent analysis of photometric $BVIJK$ light curves of the X-ray nova GU Mus using the hot-line model has yielded parameters for the system occupying a narrower range than those obtained in other studies based on standard models for close binary systems (for example, cf. [26]). Using the component-mass ratio $q = M_1/M_2 \sim 8$ and the known mass function, $f_2 = 3.01 \pm 0.15\ M_\odot$, our estimate of the orbital inclination, $i = 54° \pm 1.^\circ 3$, gives the component masses $M_X = (6.7\text{–}7.6) M_\odot$ (or $7.2^{+0.4}_{-0.5}\ M_\odot$), $M_2 = 0.93(3)\ M_\odot$. These uncertainties correspond to the 90% confidence interval. Our estimate of the uncertainty in i was obtained by running through values for this parameter keeping the remaining parameters fixed at their best-fit values.

The mass we have derived for the primary, black-hole, component is in good agreement with the values found earlier in [24, 26], whereas the mass of the secondary, a K3–4V star, is higher than the values (0.70–0.74) $M_\odot$ corresponding to main-sequence stars of this spectral type [36]. The radii of single K3–4V stars do not exceed $(0.76\text{–}0.81) R_\odot$. The radius of the secondary of the binary GU Mus coincides with the size of the star's Roche lobe, which is equal to $R_2 = 0.23 a_0$ in our case, where $a_0 = (4.80 \pm 0.14) R_\odot$ is the distance between the centers of mass of the components, i.e., $R_2 = (1.10 \pm 0.03) R_\odot$, and the secondary has obviously already left the main sequence. The secondary, whose effective temperature is 4500 K, has a bolometric luminosity of $L_{\rm bol} = (1.7 \pm 0.1) \times 10^{33}$ erg/s, or $(0.43 \pm 0.01) L_\odot$. Using the observed X-ray flux at 2–30 keV during the low state, $L_X \leq 1.5 \times 10^{32}$ erg/s [1, 23], we can estimate the component-luminosity ratio to be $L_X/L_{\rm bol} < 0.1$. This ratio is too low to give rise to an appreciable reflection effect on the secondary. The observed reflection effect is apparently due to heating by ultra-soft X-ray and ultraviolet radiation from inner parts of the disk, which are heated to 100 000–180 000 K. The nature of this radiation remains unclear, but its presence necessarily follows from our analysis of the light curves.

A considerably stronger radiation flux originates from matter in the inner parts of the disk heated to temperatures of 115 000–130 000 K (see the table). Assuming this is black-body radiation, the maximum of the spectral energy distribution for such temperatures is at soft X-ray energies ($\sim$0.05 keV). Our model assumes that this radiation originates near the radius R_1, with the value adopted in our computations being $R_1 = 0.0006 a_0$, or, using the above estimates of a_0, $R_1 \sim (2\text{–}3) \times 10^8$ cm ($R_1 \sim (90\text{–}150) R_g$ in units of the gravitational radius, R_g, for masses of $M_X \sim (6.7\text{–}7.6)\ M_\odot$). The corresponding bolometric flux is $L_b \sim (0.7\text{–}2.7) \times 10^{33}$ erg/s, and the ratio of the soft X-ray to the optical flux from the secondary will be high enough to lead to an appreciable reflection effect on the red dwarf, $L_b/L_{\rm opt} \sim 0.4\text{–}1.5$.

5. CONCLUSIONS

Due to the low optical luminosity of the stars, the contribution of the optical luminosity of the accretion disk becomes significant for X-ray novae in quiescence. It is important that, due to the existence of a

region of interaction between the disk and flow (the hot line), the contribution of this gaseous structure depends on the phase of the orbital period. This gives rise to optical and infrared variability that, combined with variations due to ellipticity effects, makes interpretation of the orbital light curve less straightforward than in the case of purely ellipsoidal variability.

We have developed a technique for computing the contribution of nonstellar components to the orbital optical and infrared variability of an X-ray nova in quiescence, based on a hot-line model. Applying this technique to the X-ray nova GU Mus = GRS 1124–68, we have demonstrated that the hot-line model can provide a good description of various features of the system's orbital optical and infrared variability, including the anomalous increase of the system's luminosity at phase $\varphi \sim 0.25$. At the same time, in some cases, the hot-spot model cannot explain the anomalous shape and amplitude of the orbital light curves of "quiescent" X-ray novae.

Our detailed analysis of the orbital optical and infrared light curves of the X-ray nova GU Mus = GRS 1124–68 using a model with an ellipsoidal optical star and an accretion disk with a hot line has enabled us to determine the parameters of the disk and hot line that give rise to the light-curve anomalies, and to obtain a trustworthy estimate of the orbital inclination, making it possible to derive a more reliable estimate of the mass of the black hole in the system. On the other hand, the variations of the characteristics of the accretion disk and hot line we have discovered lead to the need for studies of unstable phenomena occurring during mass transfer in "quiescent" X-ray novae, probably due to activity of their optical components, which have convective envelopes. It is also of interest to clarify the nature of the ultraviolet radiation emerging from central regions of the disk, whose luminosity exceeds the X-ray luminosity, L_X, and leads to a considerable reflection effect on the optical star in the GU Mus system in quiescence.

Note also that we have used a Planck approximation to describe the radiation from the disk and hot line, leading to large optical depths for both the accretion disk and the region of interaction of the flow with the circumstellar envelope of the binary, the hot line. If the optical depth of the disk and hot line for the quiescent state of GU Mus is not high, the optical variability of the nonstellar components (disk + hot line) should be less strong than we have found. In this case, the accretion disk and hot line will only provide a constant addition to the system's optical luminosity. This ambiguity can be removed using spectrophotometric estimates of the component-luminosity ratio at various phases of the orbital period. Thus, further detailed and high-accuracy spectroscopic observations of X-ray novae in their low state are very promising.

ACKNOWLEDGMENTS

This study was supported by the Russian Foundation for Basic Research (projects 02-02-16088, 02-02-16462, 02-02-17642, 03-02-16622), the State Science and Technology Program "Astronomy," the State Program "Universities of Russia—Basic Research" (grant UR.02.03.012/1), grants of the President of the Russian Federation (NS-388.2003.2, NS-162.2003.2), the Programs of the Presidium of Russian Academy of Sciences "Mathematical Modeling" and "Unstable Processes in Astronomy," and the INTAS foundation (grant 00-491).

REFERENCES

1. A. M. Cherepashchuk, N. A. Katysheva, T. S. Khruzina, and S. Yu. Shugarov, *Highly Evolved Close Binary Stars. Catalogue* (Gordon and Breach, Brussels, 1996).
2. A. M. Cherepashchuk, Space Sci. Rev. **93**, 473 (2000).
3. Y. Tanaka and N. Shibazaki, Annu. Rev. Astron. Astrophys. **34**, 607 (1996).
4. Y. Tanaka, in *Black Holes in Binaries and Galactic Nuclei*, Ed. by L. Kaper, E. P. J. van den Heuvel, and P. A. Woudt (Springer, 2001), p. 141.
5. W. Chen, C. R. Shrader, and M. Livio, Astrophys. J. **491**, 312 (1997).
6. Y. Tanaka, in *Disk Instabilities in Close Binary Systems. 25 Years of the Disk-Instability Model*, Ed. by S. Mineshige and J. C. Wheeler (Univ. Acad. Press, Kyoto, Japan, 1999), p. 21.
7. *Basic Physics of Accretion Disk,* Ed. by S. Kato, S. Inagaki, S. Mineshige, and J. Fukue (Gordon and Breach, Kyoto, Japan, 1996).
8. A. M. Cherepashchuk, Usp. Fiz. Nauk **166**, 809 (1996) [Phys. Usp. **39**, 769 (1996)].
9. P. Charles, in *Black Holes in Binaries and Galactic Nuclei,* Ed. by L. Kaper, E. P. J. van den Heuvel, and P. A. Woudt (Springer, 2001), p. 27.
10. D. V. Bisikalo, A. A. Boyarchuk, O. A. Kuznetsov, and V. M. Chechetkin, Astron. Zh. **74**, 880 (1997) [Astron. Rep. **41**, 786 (1997)].
11. D. V. Bisikalo, A. A. Boyarchuk, O. A. Kuznetsov, and V. M. Chechetkin, Astron. Zh. **74**, 889 (1997) [Astron. Rep. **41**, 794 (1997)].
12. D. V. Bisikalo, A. A. Boyarchuk, V. M. Chechetkin, *et al.*, Mon. Not. R. Astron. Soc. **300**, 39 (1998).
13. D. V. Bisikalo, A. A. Boyarchuk, O. A. Kuznetsov, *et al.*, Astron. Zh. **75**, 706 (1998) [Astron. Rep. **42**, 621 (1998)].
14. D. V. Bisikalo, A. A. Boyarchuk, O. A. Kuznetsov, *et al.*, Astron. Zh. **75**, 40 (1998) [Astron. Rep. **42**, 33 (1998)].

15. T. S. Khruzina, A. M. Cherepashchuk, D. V. Bisikalo, *et al.*, Astron. Zh. **78**, 625 (2001) [Astron. Rep. **45**, 538 (2001)].
16. T. S. Khruzina, A. M. Cherepashchuk, D. V. Bisikalo, *et al.*, Astron. Zh. **80** (2003, in press).
17. N. Lund, S. Brandt, F. Makino, *et al.,* IAU Circ. **5161**, 1 (1991).
18. F. Makino *et al.*, IAU Circ. **5161**, 1 (1991).
19. M. Della Valle, B. J. Jarvis, and R. M. West, Astron. Astrophys. **247**, L33 (1991).
20. R. A. Remillard, J. E. McClintock, and C. D. Bailyn, Astrophys. J. Lett. **399**, L145 (1992).
21. E. A. Antokhina and A. M. Cherepashchuk, Pis'ma Astron. Zh. **19**, 500 (1993) [Astron. Lett. **19** (3), 194 (1993)].
22. N. I. Balog, A. V. Goncharskiĭ, Z. Yu. Metlitskaya, and A. M. Cherepashchuk, Perem. Zvezdy **21** (155), 695 (1982).
23. J. A. Orosz, C. D. Bailyn, J. E. McClintock, and R. A. Remillard, Astrophys. J. **468**, 380 (1996).
24. J. Casares, E. L. Martin, P. A. Charles, *et al.*, New Astron. **1** (4), 299 (1997).
25. T. Shahbaz, T. Naylor, and P. A. Charles, Mon. Not. R. Astron. Soc. **285**, 607 (1997).
26. D. M. Gelino, T. E. Harrison, and B. J. McNamara, Astron. J. **122**, 971 (2001).
27. R. E. Wilson and E. J. Devinney, Astrophys. J. **166**, 605 (1971).
28. N. I. Shakura and R. A. Sunyaev, Astron. Astrophys. **24**, 337 (1973).
29. T. S. Khruzina, Astron. Zh. **78**, 298 (2001) [Astron. Rep. **45**, 255 (2001)].
30. N. G. Bochkarev, R. A. Sunyaev, T. S. Khruzina, *et al.*, Astron. Zh. **65**, 778 (1988) [Sov. Astron. **32**, 405 (1988)].
31. N. I. Shakura and R. A. Sunyaev, Mon. Not. R. Astron. Soc. **175**, 613 (1975).
32. A. A. Esin, J. E. McClintock, and R. Narayan, Astrophys. J. **489**, 865 (1997).
33. A. A. Esin, E. Kuulkers, J. E. McClintock, and R. Narayan, Astrophys. J. **532**, 1069 (2000).
34. T. S. Khruzina, Astron. Zh. **77**, 510 (2000) [Astron. Rep. **44**, 446 (2000)].
35. D. Himmelblau, *Applied Nonlinear Programming* (McGraw-Hill, New York, 1971; Mir, Moscow, 1975).
36. C. Allen, *Astrophysical Quantities* (Athlone, London, 1973; Mir, Moscow, 1977).

Translated by N. Samus'